NOAA Technical Memorandum ERL WPL-102

CAPABILITY OF SURFACE-BASED CLEAR-AIR DOPPLER RADAR FOR MONITORING REFRACTIVE INDEX GRADIENTS ALOFT

Earl E. Gossard
Russell B. Chadwick
Thomas Detman
John Gaynor

Wave Propagation Laboratory
Boulder, Colorado
September 1982

noaa NATIONAL OCEANIC AND ATMOSPHERIC ADMINISTRATION / Environmental Research Laboratories

NOAA Technical Memorandum ERL WPL-102

CAPABILITY OF SURFACE-BASED CLEAR-AIR DOPPLER RADAR FOR MONITORING REFRACTIVE INDEX GRADIENTS ALOFT

Earl E. Gossard
Russell B. Chadwick
Thomas Detman
John Gaynor

Report Prepared for the Naval Ocean Systems Center
Under Military Interdepartmental Purchase Request
N6600182MP0008. Contract Monitor: J.H. Richter

Wave Propagation Laboratory
Boulder, Colorado
September 1982

UNITED STATES
DEPARTMENT OF COMMERCE
Malcolm Baldrige,
Secretary

NATIONAL OCEANIC AND
ATMOSPHERIC ADMINISTRATION
John V. Byrne,
Administrator

Environmental Research
Laboratories
George H. Ludwig
Director

NOTICE

Mention of a commercial company or product does not constitute an endorsement by NOAA Environmental Research Laboratories. Use for publicity or advertising purposes of information from this publication concerning proprietary products or the tests of such products is not authorized.

CONTENTS

CAPABILITY OF SURFACE-BASED CLEAR-AIR DOPPLER RADAR FOR MONITORING REFRACTIVE INDEX GRADIENTS ALOFT

Earl E. Gossard, Russell B. Chadwick, Thomas Detman, and John Gaynor

ABSTRACT

There is theoretical reason to believe that gradients of refractive index in stable elevated layers can be measured by surface-based, clear-air Doppler radars, sensing backscattered power (C_n^2), height gradients of the mean horizontal wind, and width of the Doppler velocity spectrum.

In this paper the approach was to measure turbulent and mean quantities on the 300 m meteorological tower at the Boulder Atmospheric Observatory (BAO) at Erie, Colorado, USA and to examine the relationships between the turbulent and mean gradient quantities in order to evaluate assumptions for simplifying the kinetic energy and temperature balance equations. Radar measurements of Doppler spectral width were also made for comparison with tower-measured velocity spectra.

On 10 February 1982 an event occurred in which an interface between cold, dry air and relatively warm, moist air ascended across the tower at a time when the radar and all sensors (including a Lyman-α humidiometer) were operating and when the carriage was positioned midway between the 150 and 200 m levels on the tower. Data were being recorded at a 10 Hz rate. Thus this case provided an almost ideal data set. For the 10 February event the crucial simplifying assumptions about the relationships between the turbulence parameters and the mean gradients of properties were verified within the range of observational uncertainty of the tower measurements and the range of uncertainty of the universal constants of turbulence theory. It remains to be demonstrated that radars can remotely sense turbulence dissipation rate adequately by measuring the width of the Doppler spectrum. Sometimes there was good agreement between radar and tower-measured values, but sometimes they differed substantially. This was at least partly a result of physical separation of the radar and the tower, which was about 550 m.

INTRODUCTION

It is well established that sensitive ground-based radars can sense the presence of many elevated meteorological layers (see Fig. 1).

As pointed out by Gossard et al. (1982), some reasonable assumptions for simplifying the turbulent energy and variance budget equations lead to an expression relating the height-gradient of mean refractive index in elevated

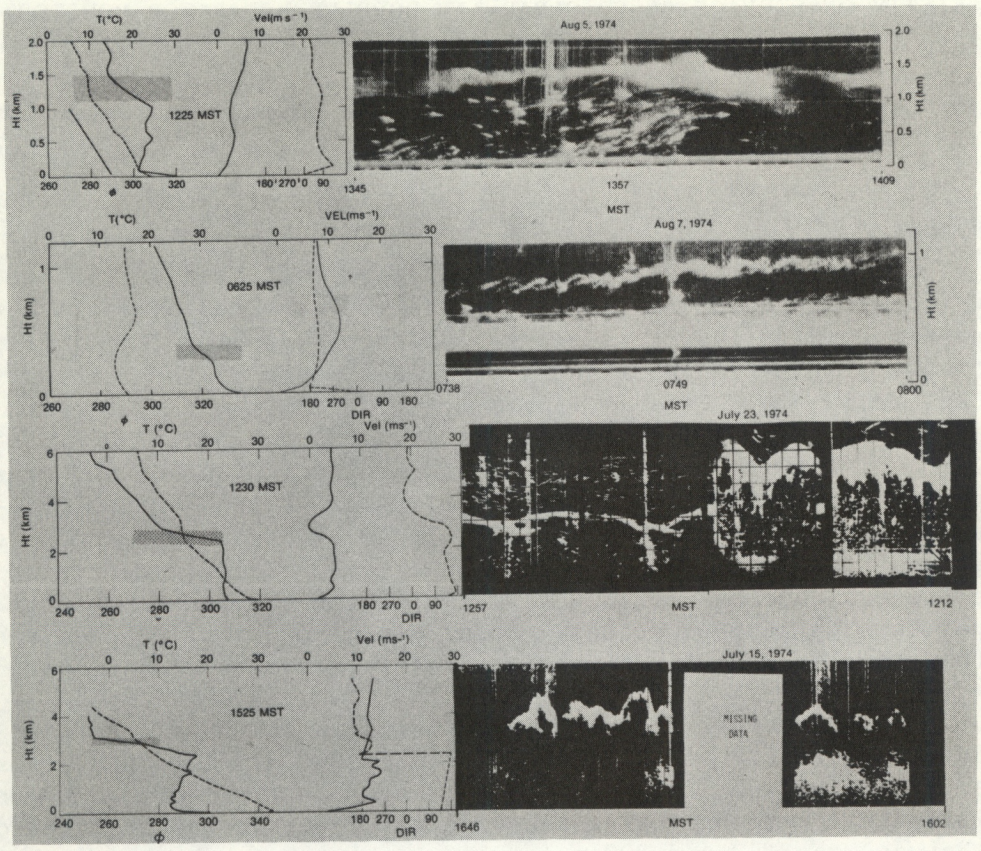

Figure 1.--Examples of radar return from elevated layers and from insect point targets. Soundings of temperature, T(°C), potential refractive index, ϕ, and wind are shown on the left.

layers to the intensity of radar backscatter, the Doppler radar-measured shear in the mean wind and the radar-measured variance in the radial wind velocity using the width (or 2nd moment) of the Doppler spectrum.

In summary,

$$C_\phi^{\,2} = B_\phi \varepsilon^{-1/3} K_\phi \left(\frac{\partial \phi}{\partial z}\right)^2$$

where,

$$\varepsilon = \left(\frac{C_v^{\,2}}{B}\right)^{3/2}$$

and,

$$K_\phi = \frac{C_v^3}{\left(\frac{\partial \bar{u}}{\partial z}\right)^2 \left[\frac{K_m}{K_\theta} - Ri\right]^{3/2} B^{3/2}}$$

whence,

$$\frac{C_v^2}{C_\phi^2} \frac{\left(\frac{\partial \phi}{\partial z}\right)^2}{\left(\frac{\partial |v|}{\partial z}\right)^2} = \frac{B}{B_\phi} \left(\frac{K_m}{K_\theta} - Ri\right) \tag{1}$$

where

ϕ is potential refractive index $= \frac{77.6}{\theta} (1000 + \frac{4810 e_p}{\theta})$

θ is potential temperature

e_p is potential vapor pressure in millibars

$d\bar{u}/dz$ is gradient of the mean wind with height

K_m/K_θ is the ratio of the eddy coefficients of momentum and heat

Ri is the gradient Richardson Number $= (g/\bar{\theta})(d\bar{\theta}/dz)(d\bar{u}/dz)^{-2}$

B, B_ϕ are universal constants whose estimated ranges are given in Table 1

C_v^2, C_ϕ^2 structure parameters whose definitions are given in Table 1.

The same reasoning that led to Eq. (1) leads to,

$$\frac{C_v^2}{C_\theta^2} \frac{\left(\frac{\partial \theta}{\partial z}\right)^2}{\left(\frac{\partial |v|}{\partial z}\right)^2} = \frac{B}{B_\theta} \left(\frac{K_m}{K_\theta} - Ri\right) \tag{2}$$

for potential temperature, whence,

$$\frac{C_\phi^2 \left(\frac{\partial \theta}{\partial z}\right)^2}{C_\theta^2 \left(\frac{\partial \phi}{\partial z}\right)^2} = \frac{B_\phi}{B_\theta} \quad . \tag{3}$$

TABLE 1.--Turbulence Parameters

Velocity Field

$$E(k) = \alpha\varepsilon^{2/3} k^{-5/3} \quad , \qquad \alpha = 1.53\text{-}1.68$$

$$S(k_1) = A\varepsilon^{2/3} k_1^{-5/3} \quad , \qquad A = 0.50\text{-}0.55$$

$$D_u(\ell) = \overline{[u(x+\ell) - u(x)]^2} = \underbrace{B\,\varepsilon^{2/3}}_{C_v^2}\,\ell^{2/3} \quad , \qquad B = 2.0\text{-}2.2 \ .$$

Refractive Index Field

$$E_\phi(k) = \alpha_\phi\, \varepsilon^{-1/3}\, \varepsilon_\phi\, k^{-5/3} \quad , \qquad \alpha_\phi = 1.33\text{-}1.67$$

$$S_\phi(k_1) = A_\phi\, \varepsilon^{-1/3}\, \varepsilon_\phi\, k_1^{-5/3} \quad , \qquad A_\phi = 0.8\text{-}1.0$$

$$D_\phi(\ell) = \underbrace{B_\phi\, \varepsilon^{-1/3}\, \varepsilon_\phi}_{C_\phi^2}\, \ell^{2/3} \quad , \qquad B_\phi = 3.2\text{-}4.0 \ .$$

There is no physical reason to suggest that B_ϕ/B_θ is not unity, so (3) says that

$$C_\phi^2 \propto \left(\frac{\partial\theta}{\partial z}\right)^2 \quad \text{and} \quad C_\theta^2 \propto \left(\frac{\partial\theta}{\partial z}\right)^2$$

and that the proportionality constants are the same. This is just the reasonable statement that the power in the fluctuations is determined by the square of the gradient of the quantity for a given turbulent intensity, and that the turbulent intensity interacts with the mean gradients to create variance the same way for both θ and ϕ. However, length scales are defined by (see Tatarski, 1971, pg. 72),

$$\frac{C_\phi^2}{\left(\frac{\partial\phi}{\partial z}\right)^2} = L_\phi^{4/3}, \quad \frac{C_\theta^2}{\left(\frac{\partial\theta}{\partial z}\right)^2} = L_\theta^{4/3}, \quad \frac{C_v^2}{\left(\frac{\partial|v|}{\partial z}\right)^2} = L_v^{4/3} \qquad (4)$$

so that (3) gives,

$$\left(\frac{L_\phi}{L_\theta}\right)^{4/3} = \frac{B_\phi}{B_\theta} = 1 .$$

The length scales so defined are simply the vertical distance δ, thru which a parcel must be mixed in a given gradient to cause a perturbation (variance) at its new level equal to the variance of the structure function for homogeneous, isotropic turbulence corresponding to a separation length equal to δ. Thus, it is a "mixing length," but it is more quantitatively defined than the classical Prandtl Mixing Length. Similarly,

$$\frac{C_v^2}{C_\theta^2} \frac{\left(\frac{\partial\theta}{\partial z}\right)^2}{\left(\frac{\partial|v|}{\partial z}\right)^2} = \frac{L_v}{L_\theta}^{4/3} .$$

While it is unlikely that $L_v/L_\phi = 1$, it seems reasonable to hypothesize that the ratio is constant because the same eddy ensemble is mixing both heat and momentum; i.e., that static stability and shear (the Ri) effect the mixing of both in the same way. If so, Eq. (2) shows that (K_m/K_θ)-Ri = constant, and the problem is greatly simplified because Eq. (1) then gives,

$$\left(\frac{\partial\bar{\phi}}{\partial z}\right)^2 = \frac{B}{B_\phi}\left[\frac{C_\phi^2(\partial|v|/\partial z)^2}{C_v^2}\right] \text{x constant} \qquad (5)$$

and the radar can, in principle, measure all the quantities in braces. Since the tower is instrumented to measure all of the parameters in (5) (as well as C_θ^2, $d\theta/dz$, C_q^2 and dq/dz), the relationships between quantities can be checked. The procedure, then, was to compare measured,

$$C_\phi^2(\partial\bar{v}/\partial z)^2/C_v^2 \text{ with } (\partial\bar{\phi}/\partial z)^2$$

or, alternatively,

$$C_v^2(\partial\bar{\phi}/\partial z)^2/(\partial\bar{v}/\partial z)^2 \text{ with } C_\phi^2 .$$

Actually, more direct comparisons can be made between $C_\theta^2(\partial\bar{v}/\partial z)^2/C_v^2$ and $(\partial\theta/\partial z)^2$ or $C_\theta^2(\partial\bar{q}/\partial z)^2/C_q^2$ and $(\partial\bar{\theta}/\partial z)$ because ϕ is a quantity calculated from temperature and humidity, whereas temperature and humidity are direct measurables. It is the comparison of the gradients of temperature with the wind field that is important in the present application, because of the ability of the radar to measure $C_N^2 \simeq C_\phi^2$, C_v^2 and $d\bar{v}/dz$, whereas it cannot directly measure the corresponding quantities for θ and q. In the cases analyzed, directional shear in the mean wind is as important as speed shear, so it is shear in the vector wind that is important. Figure 2 shows that,

$$\left|\frac{\partial \underset{\sim}{v}}{\partial z}\right| = \sqrt{\left(\frac{\partial u}{\partial z}\right)^2 + \left(\frac{\partial v}{\partial z}\right)^2}$$

is the important shear quantity, and it was used in the calculations.

The measurements were especially suitable for comparison of time series, because the carriage remained at a fixed level while the layer progressed upward across it. However, an effort was made to deduce height profiles also by interpolating turbulent parameters between fixed levels at all heights.

Experimental Set-Up

The 300 m tower (Fig. 3) is instrumented at 8 levels (10, 22, 50, 100, 150, 200, 250, and 300 m) with fast response sensors (see Fig. 4), such as platinum wire thermometers, sonic anemometers and a Lyman α humidiometer (only on the carriage) and with accurate, but slow response, sensors such as quartz thermometers, prop-vane anemometers and dew pointers. These are distributed on the ends of two booms at each fixed level as shown in Fig. 5 and on a carriage that can be run up and down the tower configured as shown in Fig. 6. Thus, quantities such as C_θ^2, C_q^2, and C_v^2 are obtained from the power spectra of time series recorded by the platinum wire, Lyman α and sonic sensors, respectively, and the gradient quantities are obtained from the quartz, dew point and prop-vane sensors. As shown in Fig. 6 the carriage was placed midway between two fixed levels (150 and 200 m) at a height of 175 m. The gradients were obtained from measurements at the two fixed levels and the turbulent

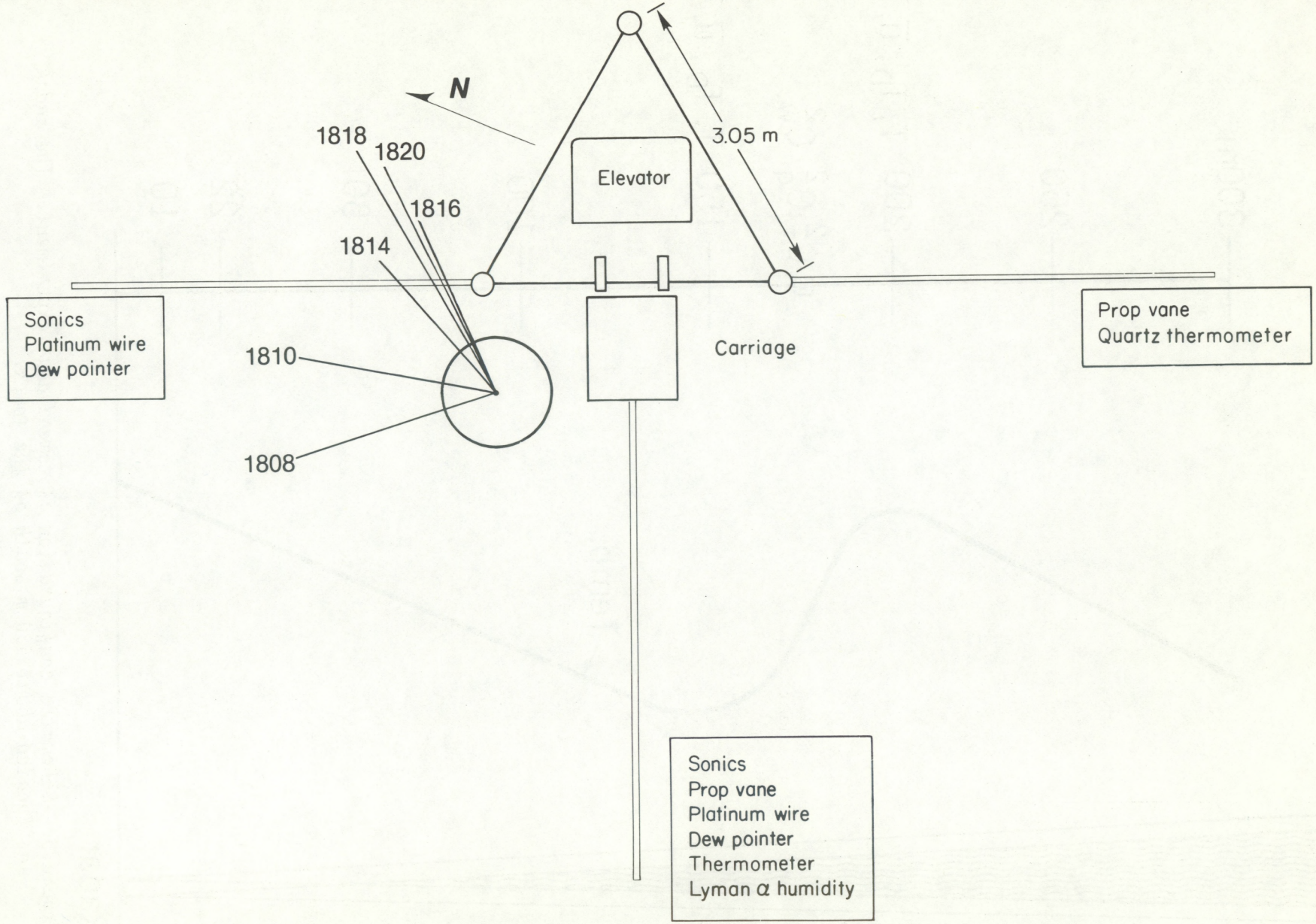

Figure 2.--Configuration of booms on the BAO tower and their instrumentation.

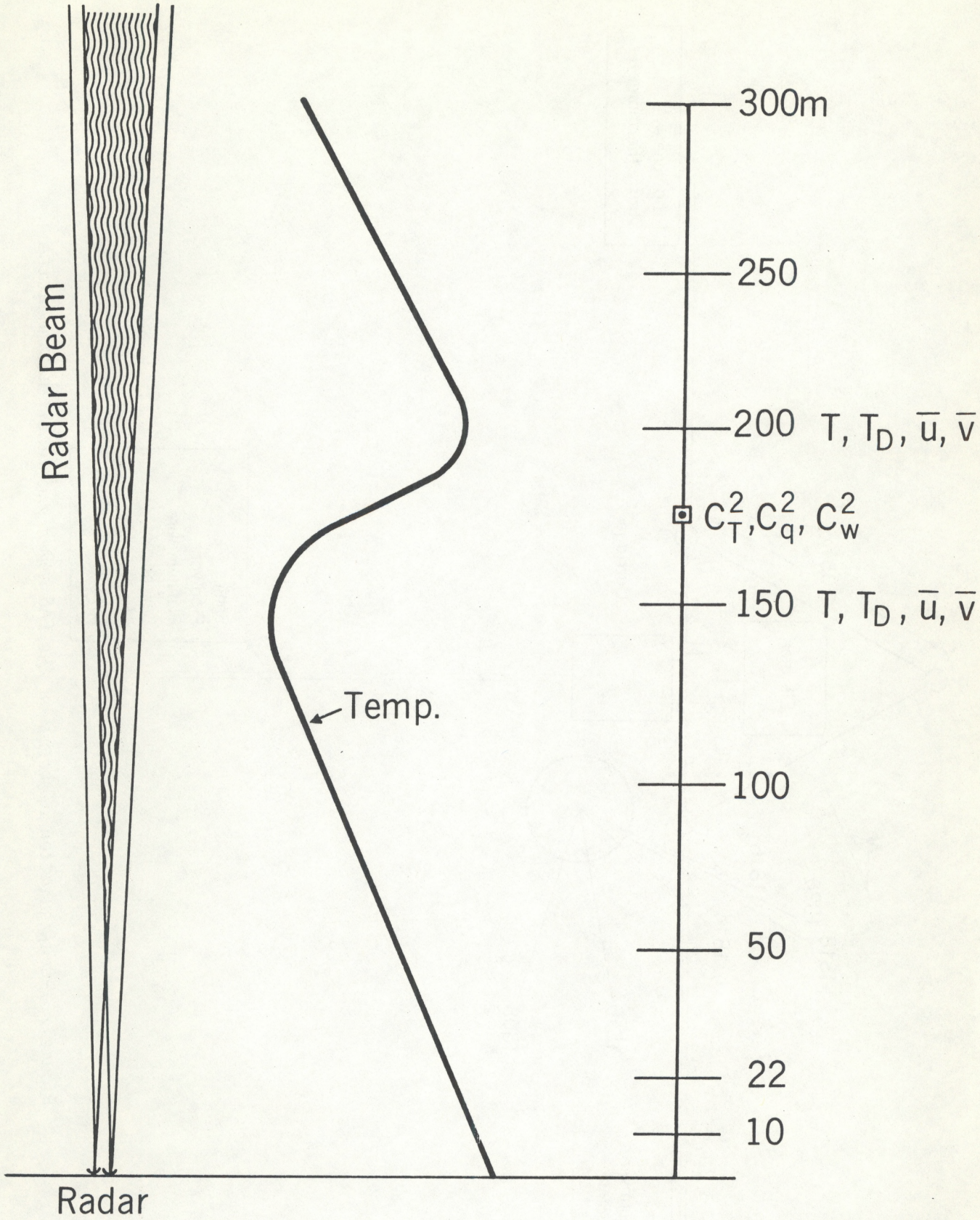

Figure 3.--Schematic configuration of tower/radar experiment. The radar was located about 550 m south of the tower.

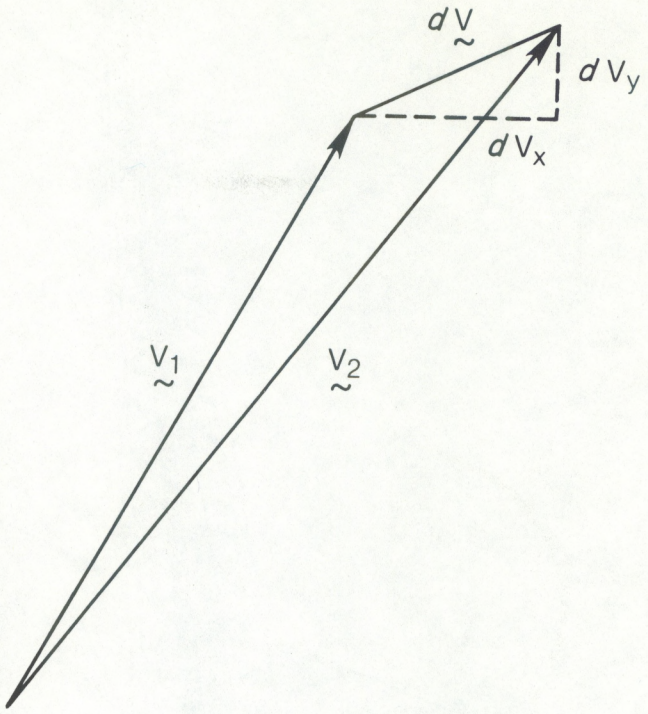

$$\left| d\underset{\sim}{V} \right|^2 = (dV_x)^2 + (dV_y)^2$$

$$Ri = \frac{g}{\overline{T}} \frac{\frac{\partial \theta}{\partial z}}{\left(\frac{\partial V_x}{\partial z}\right)^2 + \left(\frac{\partial V_y}{\partial z}\right)^2}$$

Figure 4.--The Richardson Number when directional wind shear is present.

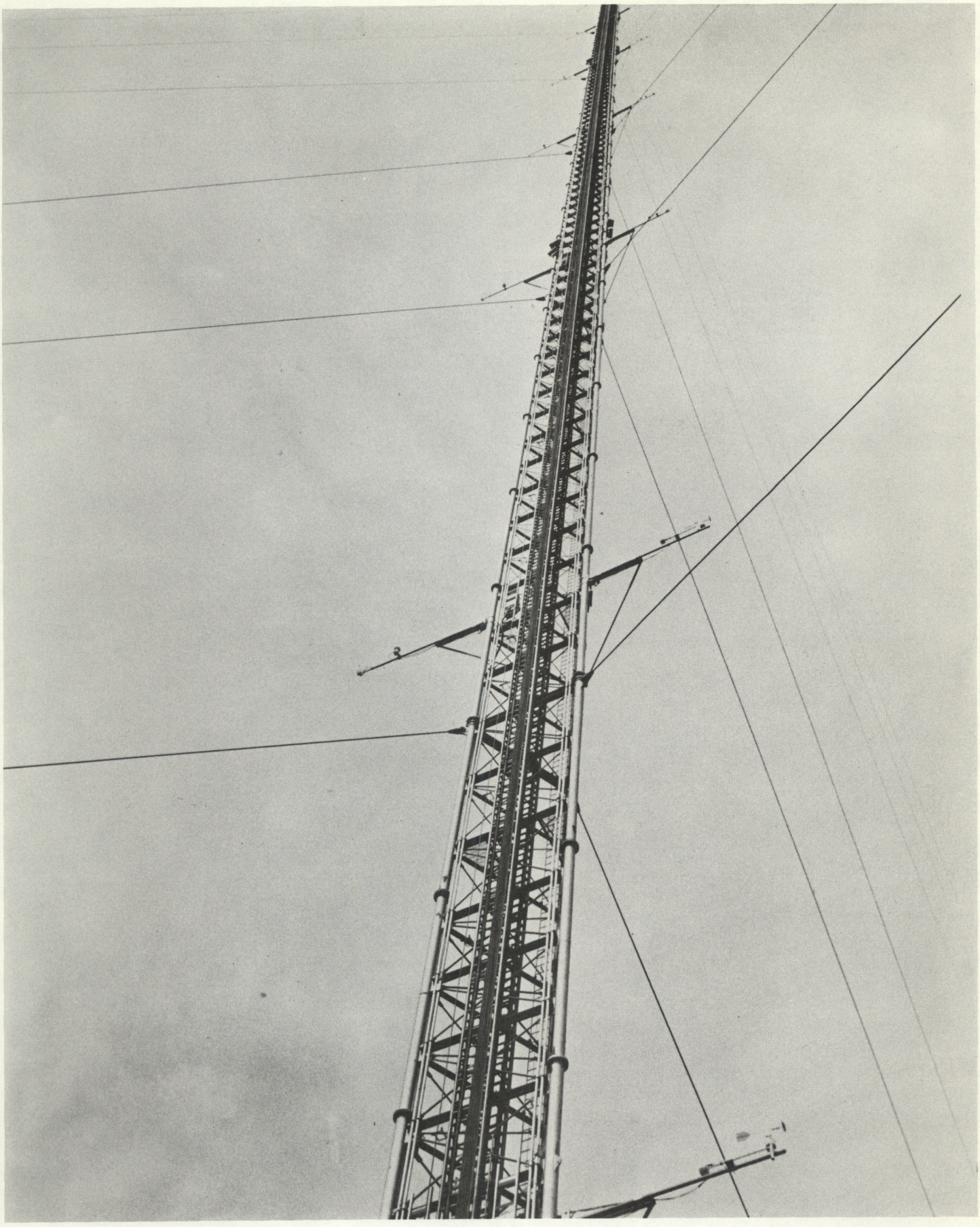

Figure 5.--The 300 m tower of the Boulder Atmospheric Observatory.

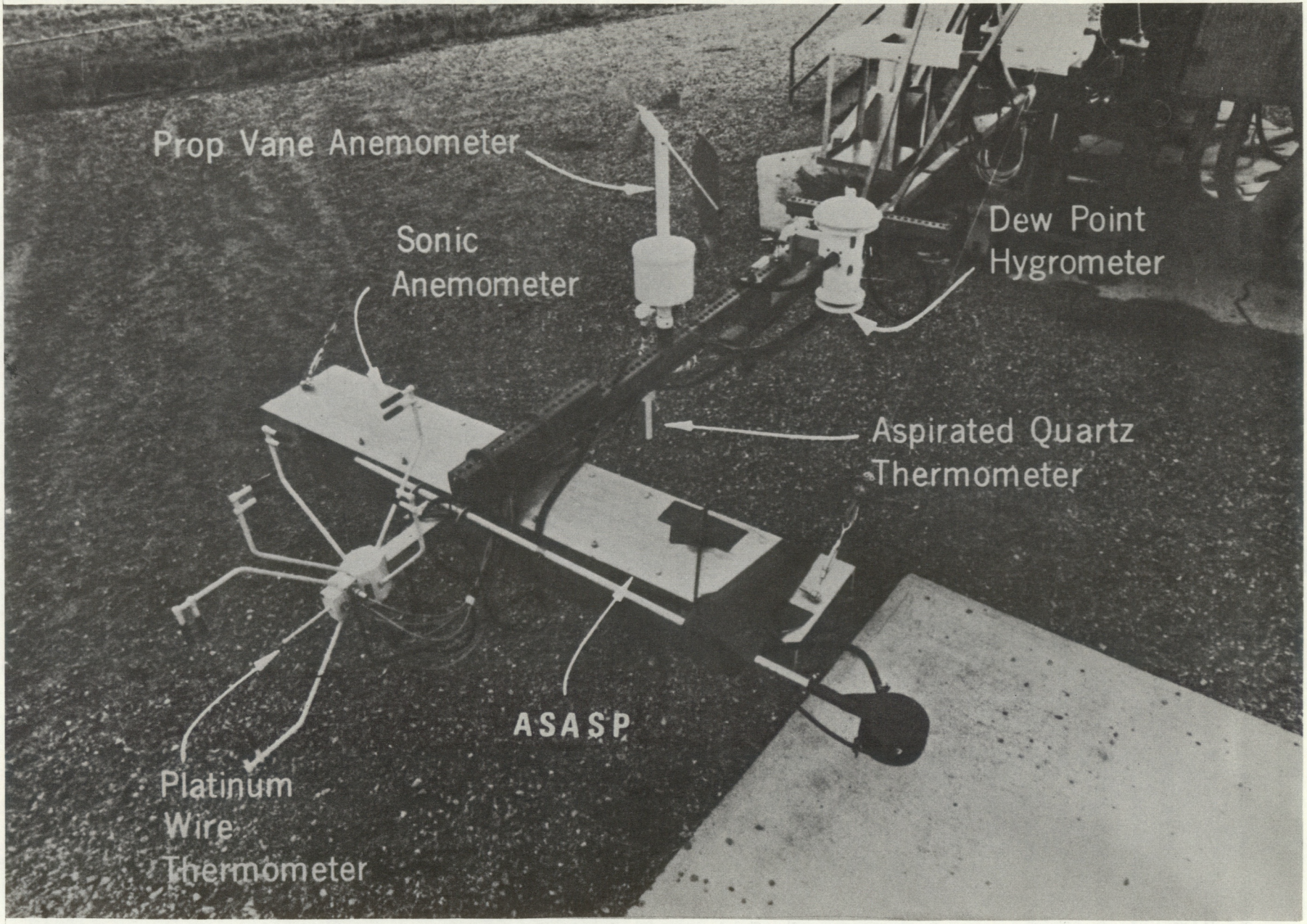

Figure 6.--Instrumentation on the carriage boom.

quantities were measured on the carriage boom midway between. C_v^2 was actually obtained from the sonic anemometer spectrum of vertical velocity after it was verified that $C_u^2 = C_v^2 = C_w^2$ as would be expected if the turbulence were isotropic at the high wavenumbers of the inertial subrange. Typical spectra are shown in Fig. 7, where the values of $C_u^2 \simeq C_w^2 \equiv B^{2/3}$ were evaluated at the frequencies indicated. The power in the inertial subrange, and therefore C_w^2, was arbitrarily evaluated at a wavenumber of one corresponding to the frequency, f_o, found from the mean horizontal wind at that level; i.e., $f_o = \frac{\bar{v}}{2\pi}$. Then, noting that $kS(k) = fS(f)$ where k is wavenumber,

$$C_w^2 = \frac{B}{A} f_o S(f_o), \quad \varepsilon = \left[\frac{f_o S(f_o)}{A}\right]^{3/2} \tag{6}$$

where ε is turbulent dissipation rate and best estimates of A and B are given in Table 1. After calculating f_o, the ordinate value $\log f_o S(f_o)$ is simply read off of spectra such as Fig. 7 and C_w^2 and ε are calculated from (6). The ordinate values are read from lines with a slope of -2/3, drawn through each spectrum, which are a best fit to the high frequency (inertial subrange) portion of the spectrum. Note that a spectrum of form $f^{-5/3}$ yields a straight line with a -2/3 slope on a log log plot when fS(f) is plotted against f. It is the highest frequency portion of the spectrum that is important for comparison with the radar because radar backscatter from the clear air depends on turbulence scales equal to $\lambda/2$, where λ is radar wavelength. The temperature structure parameter C_θ^2 was calculated as described for C_v^2, except the temperature spectrum was used instead of velocity, i.e.,

$$C_T^2 = \frac{B_T}{A_T} f_o S_T(f_o), \quad \varepsilon_T = \frac{f_o S_T(f_o)}{A_T \varepsilon^{-1/3}} \tag{7}$$

where ε_T is rate of "dissipation" of temperature variance (actually half variance, or $\overline{T^2}/2$.

In addition to the length scales defined by (4), other classical turbulence lengths often discussed can be calculated from the data set with which we work here. That is:

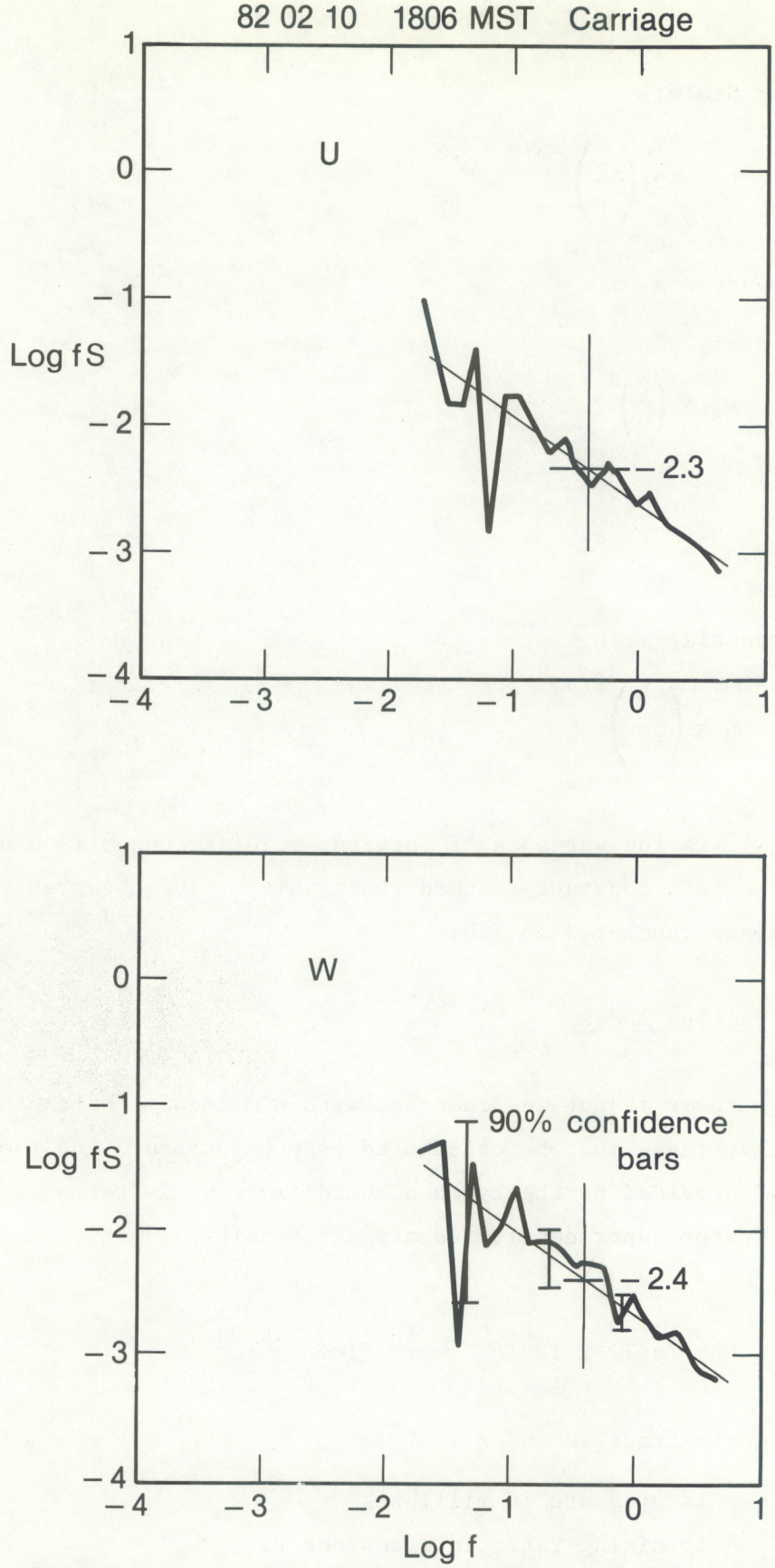

Figure 7.--Examples of velocity spectra with 90% confidence bars from sonic anemometers. Illustrates isotropy at large wavenumbers.

The Outer Scale:

$$L_o = 2\pi\left(\frac{2\alpha}{3}\right)^{-3/2} \frac{\overline{w'^2}}{\varepsilon} \tag{8}$$

The Buoyancy Scale:

$$L_B = \left(\frac{2}{c}\right)^{3/4} \pi \frac{\varepsilon^{1/2}}{N^{3/2}} \tag{9}$$

where, $N^2 = \frac{g}{\bar{\theta}} \frac{\partial\theta}{\partial z}$

The Microscale:

$$\eta = \left(\frac{\nu^3}{\varepsilon}\right)^{1/4} \tag{10}$$

In the above $\overline{w'^2}$ is the variance of vertical velocity and ν is kinematic viscosity and c is a constant assumed to be unity. The observed values of these lengths are tabulated in Table 2.

The Radar Refractive Index

The 300 m tower is not instrumented with a microwave refractometer, so radar refractive index must be calculated from temperature and the humidity "mixing ratio" provided by the Lyman α humidiometer. In terms of mixing ratio (the ratio of water vapor density to dry air density),

$$N \equiv (n-1) \times 10^6 = \frac{77.6p}{T}\left(1 + \frac{4810q}{\varepsilon T}\right) \tag{11}$$

where ν is radar refractive index,

p is pressure in millibars

q is mixing ratio in grams per kg

T is temperature in K

$\varepsilon = 0.622$

TABLE 2.--Observed Turbulence Quantities and Scales

Time (MST)	1810	1812	1814	1816
Ri	0.475	0.663	0.429	0.587
L_o(m)	288.0	401.0	4.8	21.8
L_B(m)	69.0	48.0	93.0	59.0
L_θ(m)	8.1	9.9	11.4	1.2
L_v(m)	6.7	7.0	8.4	6.7
L_θ/L_v	1.2	1.4	1.4	0.18
B_θ	2.76	5.11	4.97	0.92
$\varepsilon(cm^2\ s^{-3})$	9.7	9.7	54.7	13.8
η(cm)	0.123	0.112	0.079	0.112

It is convenient to define a "potential refractive index" ϕ analogous to potential temperature so that we can work with a quantity conserved in adiabatic motion, which is a good assumption for the time and space scales characteristic of the turbulent inertial sub-range. Referring (11) to a pressure level of 1000 mb and writing in terms of potential temperature θ where $\theta = T\,(1000/p)^{.286}$, and defining mixing ratio as grams per kg,

$$\phi = \frac{77600}{\theta} (1 + \frac{7.73q}{\theta}) \qquad (12)$$

At any level the perturbations of ϕ and θ are small compared with the mean magnitude so, writing $\phi = \phi_o + \phi'$, $\theta = \theta_o + \theta'$ and $w = w_o + w'$,

$$\phi' \simeq -a\theta' + bq' \qquad (13)$$

where for the data analyzed in this report,

$$a = \frac{77600}{\theta_o^2} + 1.2 \times 10^6 \frac{q_o}{\theta_o^3} \simeq 1.04$$

$$b = \frac{6.0 \times 10^5}{\theta_o^2} \simeq 7.23 \ .$$

Similarly, from (11),

$$N' = -a_N T' + b_N q' \tag{14}$$

where

$$a_N = \frac{77.6p}{T_o^2} + \frac{1200pq_o}{T_o^3} \simeq 0.96$$

$$b_N = \frac{600p}{T_o^2} \simeq 6.68 \quad .$$

It follows that,

$$\overline{\phi'^2} \simeq a^2 \overline{\theta'^2} + b^2 \overline{q'^2} - 2ab \overline{q'\theta'} \tag{15a}$$

and

$$\overline{N'^2} = a_N^2 \overline{T'^2} + b_N^2 \overline{q'^2} - 2a_N b_N \overline{q'T'} \tag{15b}$$

where

$$a^2 \simeq 1.08, \; b^2 \simeq 51.8, \; 2ab = 15.0$$

$$a_N^2 \simeq 0.92, \; b_N^2 \simeq 44.9, \; 2a_N b_N = 12.9 \; .$$

Furthermore, recalling that the power spectrum is the Fourier Transform of the autocovariance function, 15a,b shows that (Gossard, 1960),

$$S_\phi \simeq a^2 S_\theta + b^2 S_q - 2abS_{q\theta} \tag{16}$$

where S_ϕ, S_θ, and S_q are the power spectra of potential refractive index, potential temperature and mixing ratio, and $S_{q\theta}$ is the cross-spectrum (co-

spectrum) between temperature and humidity. Furthermore, from Table 1, S_ϕ and C_ϕ^2 are related as,

$$S_\phi = \frac{A_\phi}{B_\phi} C_\phi^2 k^{-5/3} \tag{17}$$

where A_ϕ and B_ϕ are the universal constants whose estimated values are given in Table 1. Therefore C_ϕ^2, C_θ^2, and C_q^2 are related as in Eq. (16) and values of C_N^2 and C_ϕ^2 were calculated from measured values of S_T^2 and S_q^2 using Eqs. (6) and (17), and in the figures these values of C_N^2 have been called "measured". The power spectra calculated from Eq. 16 are shown in Fig. 8 where the carriage measurements of S_q and S_θ were used to calculate S_ϕ. The importance of the co-spectrum $S_{q\theta}$ is illustrated by Fig. 9 where the power spectra with and without the contribution of the cross-power spectrum is shown along with the coherence between θ and q. Extrapolating out to a frequency of 37 Hz (which corresponds to the 5 cm turbulence length scale that is effective in the backscatter of 10 cm radar waves) we see that the co-spectrum probably remains very important at the Bragg scale for our radar. The coherence was calculated from,

$$\text{Coh} = \left(\frac{C_{\theta q}^2 + Q_{\theta q}^2}{S_q S_\theta} \right)^{1/2}$$

where $C_{\theta q}$ and $Q_{\theta q}$ are the co and quadrature spectra respectively.

The Case of 10 February 1982

In the climatic regime of Boulder strong elevated layers only rarely occur at tower levels where measurements of the kind described above can be made. On 10 February 1982, a relatively strong layer was recorded by the radar as it traversed the tower. The radar was operating unmanned, pointing vertically, and it cycled automatically between the Doppler mode and the backscattered-powervs-range mode every minute; i.e., 15 sec in Doppler and 45 sec in range-power (see Fig. 10). Furthermore, at the time of this event the carriage was instrumented with the Lyman α sensor and was at the 175 m level.

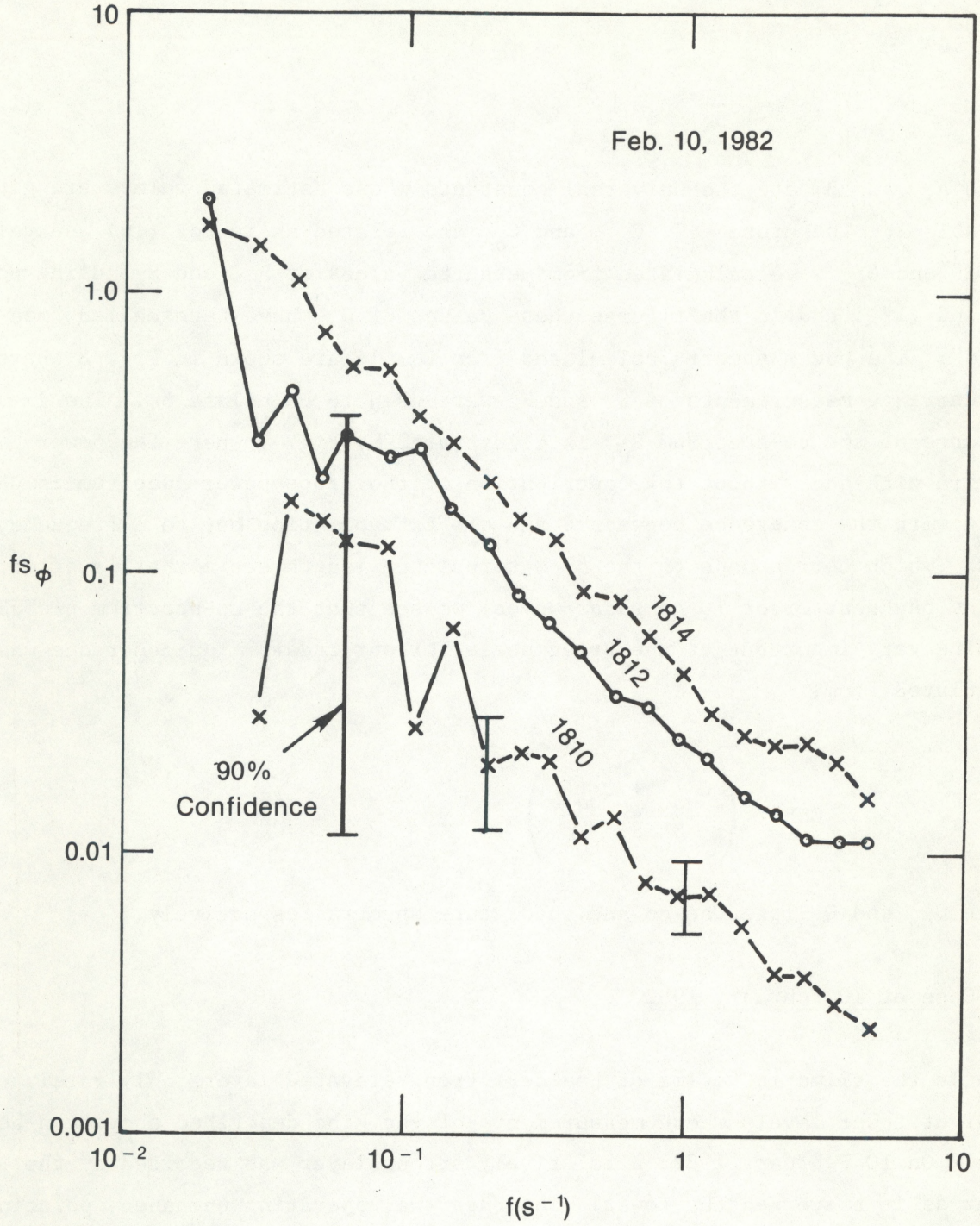

Figure 8.--Spectra of potential refractivity measured by platinum wire and Lyman α humidiometer. Ordinate is power density times frequency.

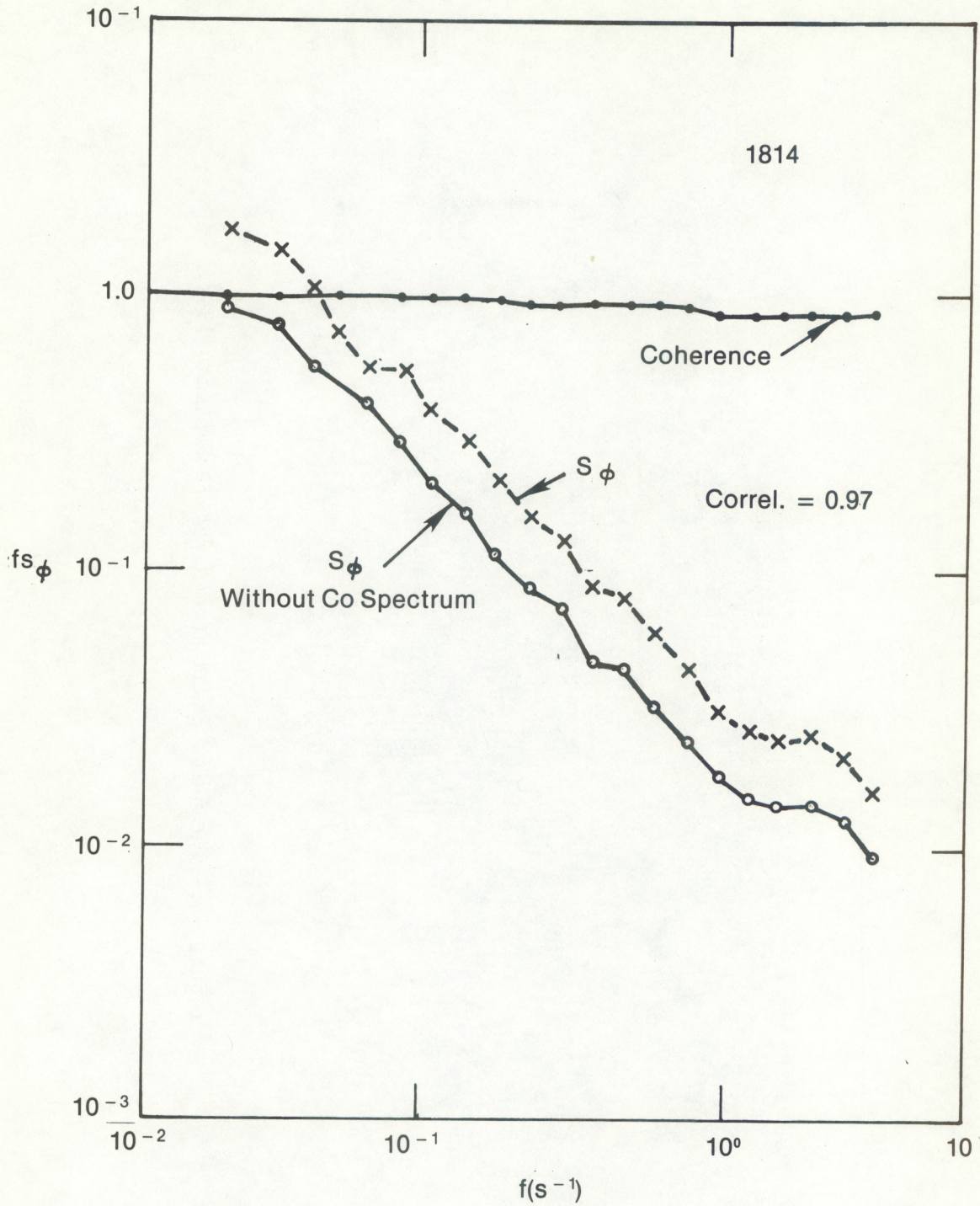

Figure 9.--Spectrum of potential refractivity with and without the contribution of the cospectrum.

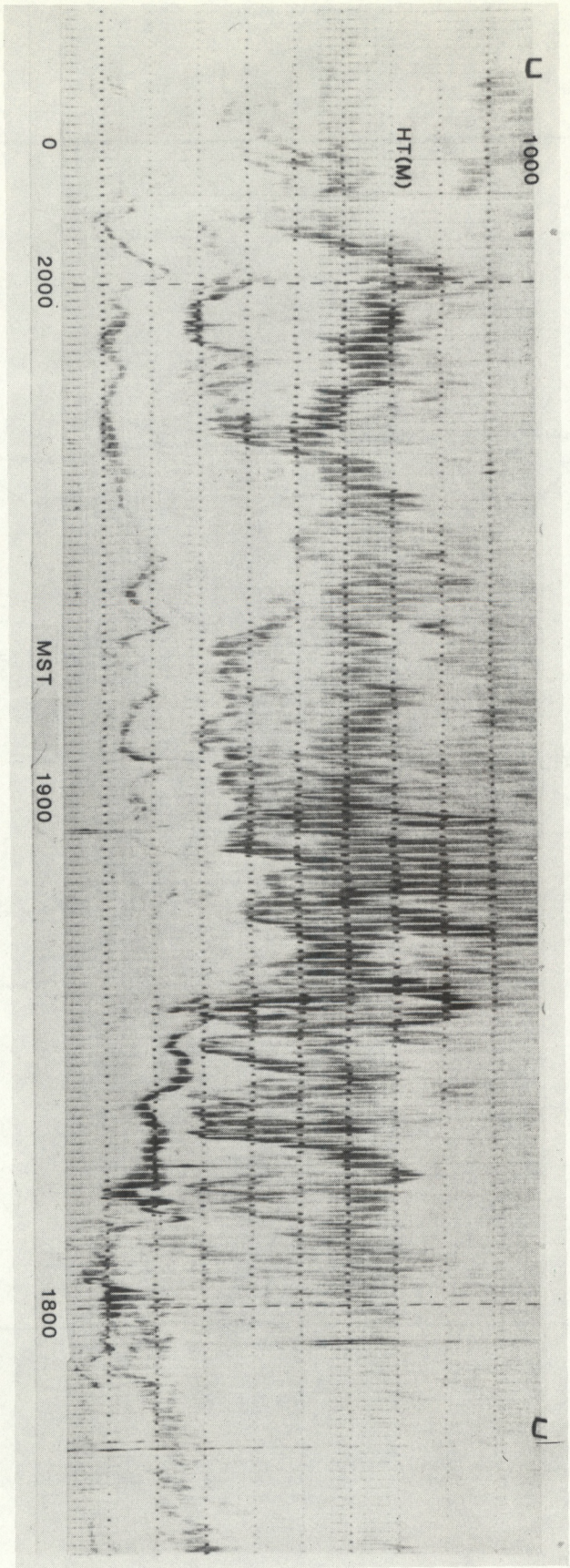

Figure 10.--The FM-CW radar record for 10 February 1982.

This coincidence is rare because the Lyman α humidometer is only mounted on special occasions, as it must be recalibrated frequently due to drift. Also, the raw 10 Hz data was being recorded at this time so that the spectra extended up to a frequency of 5 Hz (the Nyquist frequency). By contrast, the usual mode of operation only archives data at a sampling rate of 10 sec. For all of these reasons, this rare data set was analyzed intensively.

The time series of temperature and humidity are shown in Fig. 11 as the layer traversed the 175 m level. The profiles of temperature, wind and deware shown in Fig. 12. The height gradients calculated from the turbulent quantities of wind and wind gradient during this time period were compared with the measured values of height gradient from observations at the 150 m and 200 m levels bracketing the 175 m level where the turbulent measurements were made. The gradients were measured using the very accurate (but slow response) quartz thermometers and dewpointers for temperature and humidity, and the turbulence quantities were measured with the platinum wire thermometer, Lyman α humidometer and sonic anemometers on the carriage.

Figure 13 shows calculated vs. measured gradients of potential temperature during the period. Unfortunately, a wind shift accompanied the event, so, as shown by the radial line segments representing wind direction in Fig. 5, the wind swung into a northeasterly direction that brought tower-generated mechanical turbulence to the carriage instruments after 1814. Therefore, it was necessary to use turbulence quantities from the 150 m and 200 m levels after 1814, and the averaged values for these levels are shown for 1816 and 1818 in Figs. 13 and 14. In Fig. 13 the agreement in the values of height gradient of θ deduced from the turbulent humidity functions and humidity gradient [using $d\theta/dz = (d\bar{q}/dz)\ (C_T/C_q)$] is quite remarkable for the carriage turbulence values but, as is to be expected, the agreement is not so good with the averaged fixed-level values calculated for 1816 and 1818. However, the height gradient values deduced from the wind field [using $d\theta/dz = (d|\tilde{v}|/dz)(C_T/C_w)$] lie above both the observed gradient values and those calculated from humidity. Using the carriage values, the adjustment required to bring the wind field values into agreement with the others would require [see Eq. (4)],

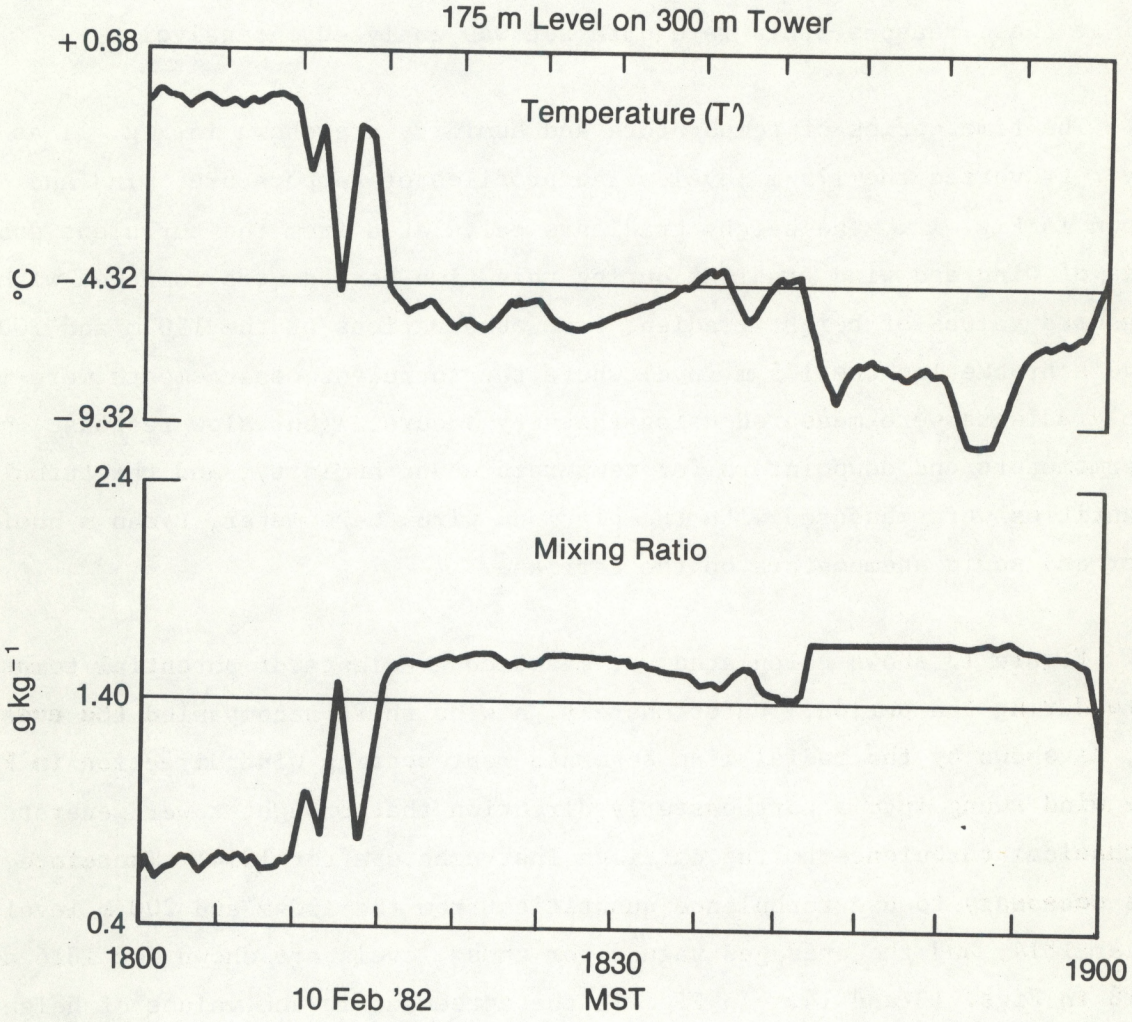

Figure 11.--Time series of temperature and humidity as the layer ascended by the carriage.

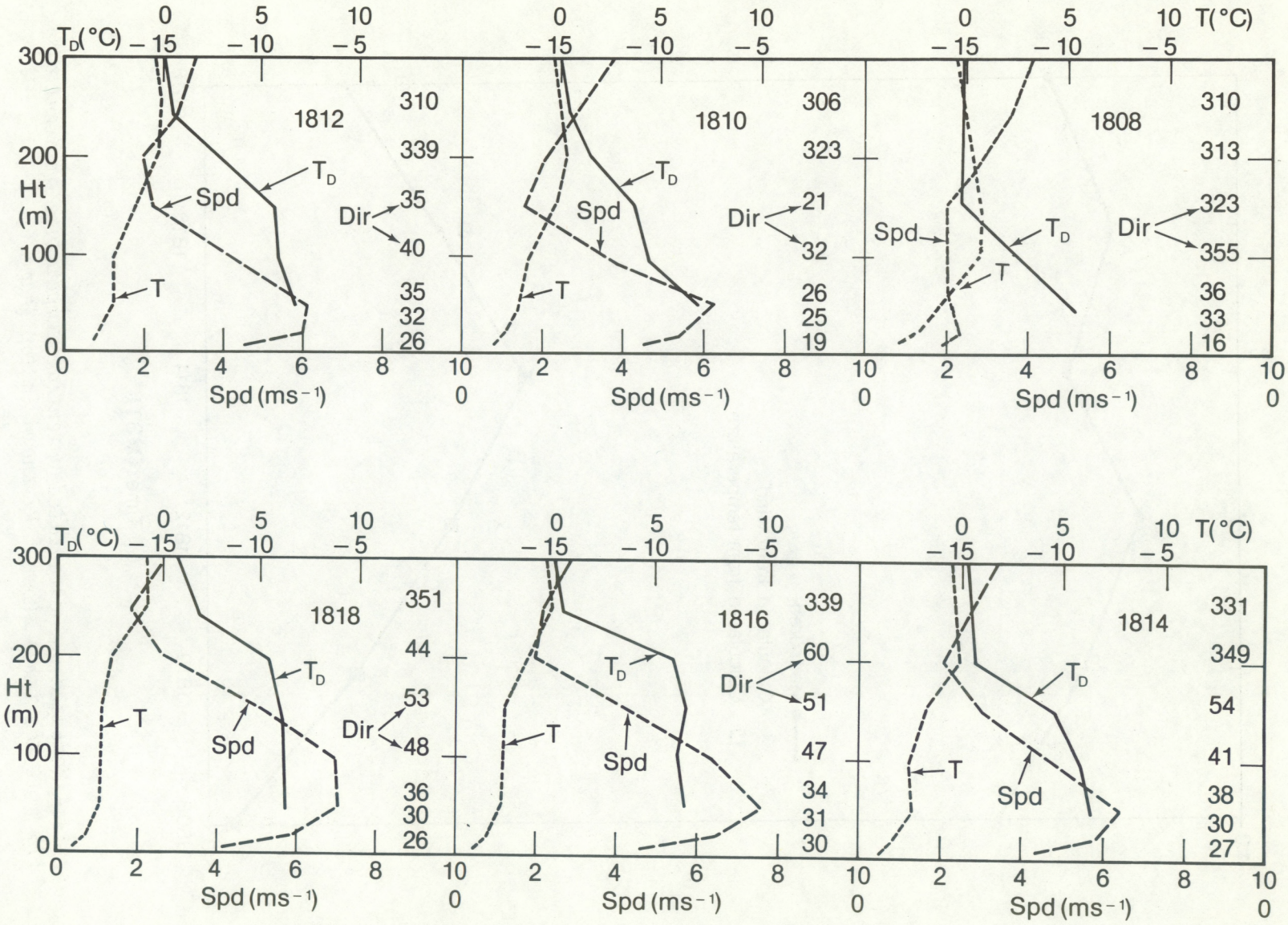

Figure 12.--Meteorological profiles across the tower at the times shown on 10 February 1982.

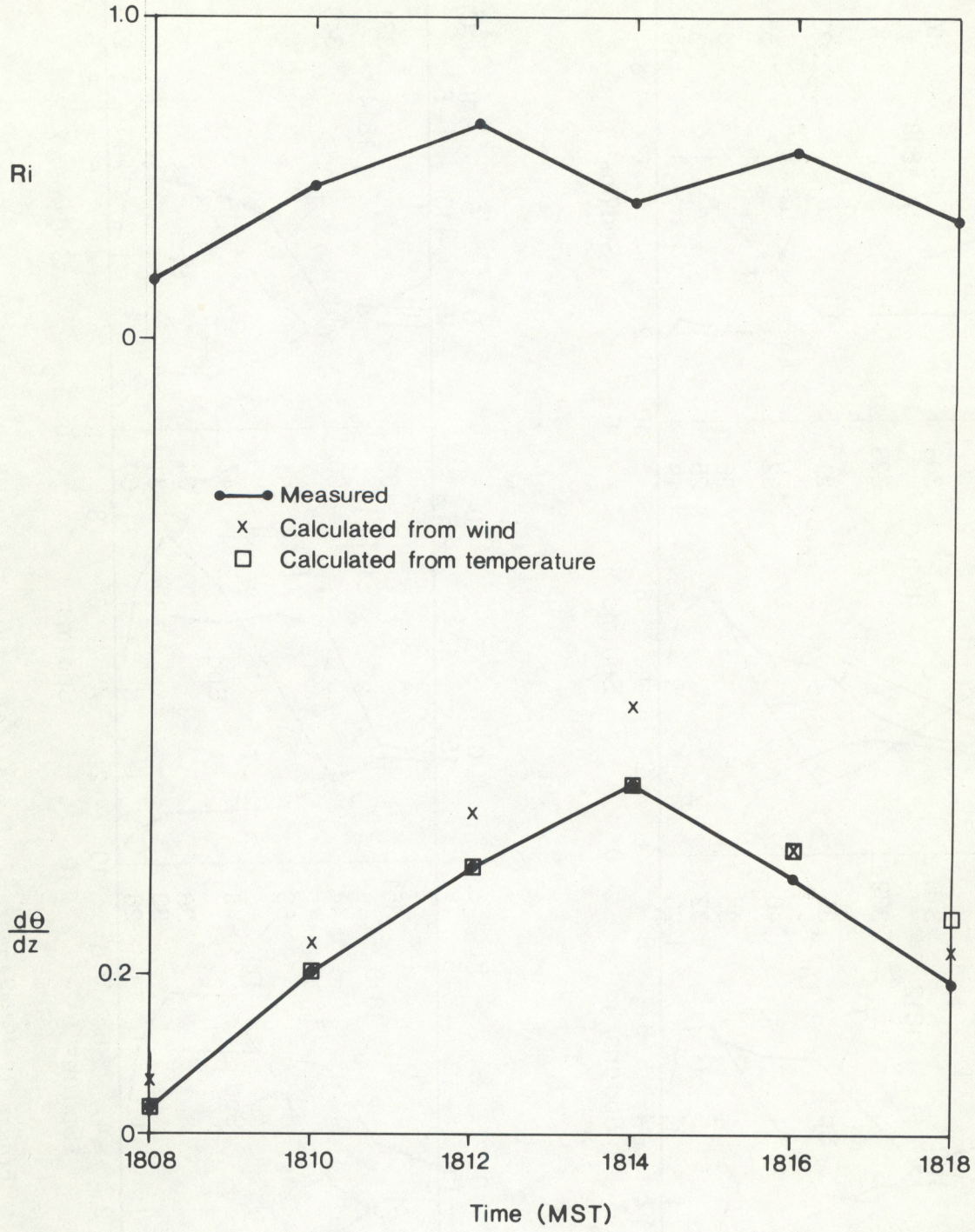

Figure 13.--Measured vs. calculated potential temperature gradient at 175 m at the times shown. Ri shown in top frame.

$$\frac{B}{B_\theta} \times \text{constant} = 0.67$$

and from Eq. (2) this means that,

$$\frac{B}{B_\theta} \frac{K_m}{K_\theta} = 0.67$$

under neutral conditions when Ri = 0. If the values of B and B_θ in the center of their range of estimate shown in Table 1 are used, this means that,

$$\frac{K_m}{K_\theta} = 1.14$$

under neutral conditions. Alternatively, if it is assumed that $K_m/K_\theta = 1$ under neutral conditions (a common assumption),

$$\frac{B_\theta}{B} = 1.5$$

which lies within the range of estimate. Thus, the hypotheses on which the calculations are based are nicely supported by this case.

Similar comments can be made regarding the refractive index gradient displayed in Fig. 14. In this case the gradient of refractive index was calculated from the temperature field [using $d\phi/dz = (d\bar{\theta}/dz)(C_N/C_T)$] and from the wind field [using $d\phi/dz = (d|\underset{\sim}{v}|/dz)(C_N/C_w)$] and compared with the measured value of $d\bar{\phi}/dz$ (solid curve). Again, the agreement between the observed gradient of ϕ and that deduced from the temperature field is quite remarkable for the carriage-measured values (through 1814). As with θ, the values deduced from the wind field lie above the measured values and by about the same amount as for θ, so if $K_m = K_\theta$ when Ri = 0,

$$\frac{B_\theta}{B} \simeq 1.5 \ .$$

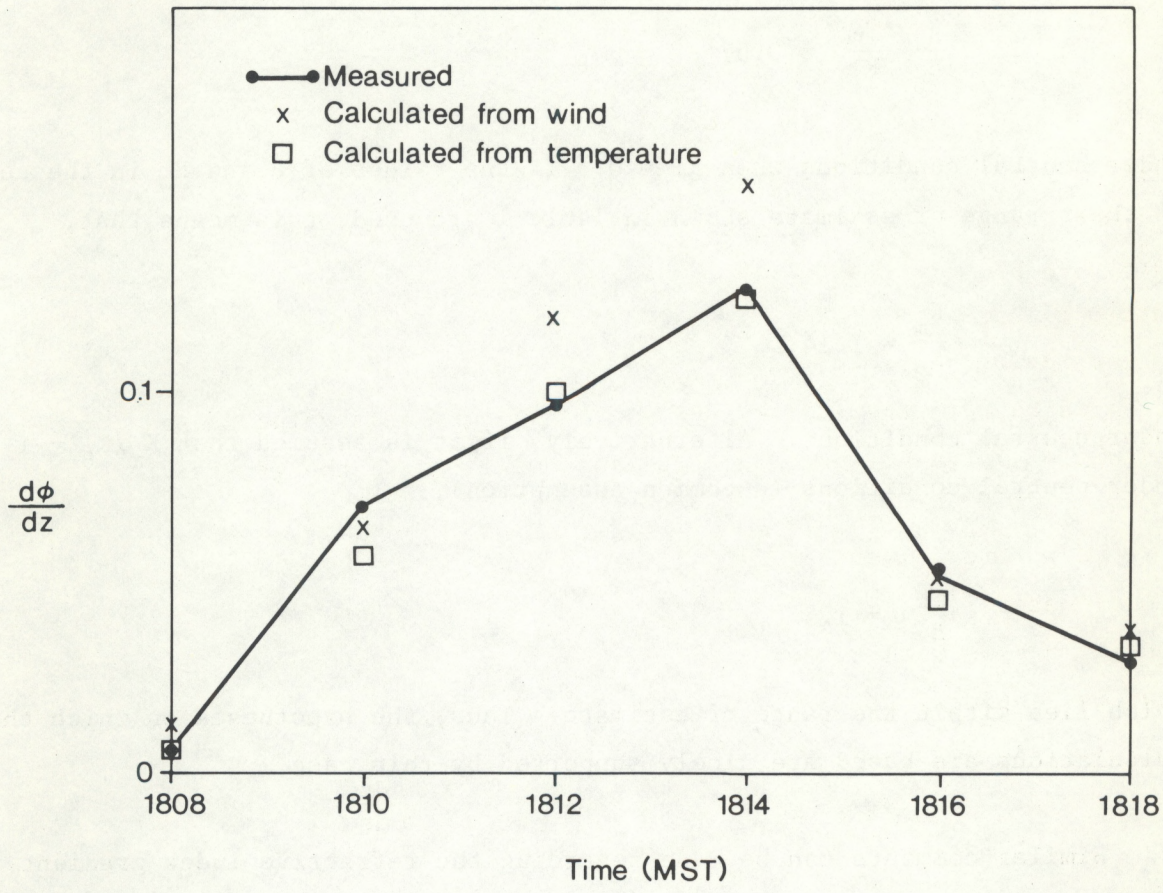

Figure 14.--Measured vs. calculated potential refractivity gradient at 175 m at the times shown.

Height profiles of $d\theta/dz$ can also be plotted if pairs of turbulence values at the fixed levels on the tower are averaged to arrive at an estimate of values midway between measurement levels. Figure 15 shows values of $d\theta/dz$ calculated from the relationship,

$$\frac{d\theta}{dz} = \sqrt{\left(\frac{du}{dz}\right)^2 + \left(\frac{dv}{dz}\right)^2} \qquad \left(\frac{\bar{C}_T}{\bar{C}_w}\right) \tag{18}$$

where the winds at the fixed levels were used to calculate height gradients and the values of $\bar{C}_\theta$ and $\bar{C}_w$ are averaged between pairs of fixed levels and were used as estimates of the value at the center of the layer between measurement levels. At the 175 m level there are also carriage values of C_w and C_T for comparison with the averaged values. As shown by Fig. 15, the differences between the average values and the measured value can be large in regions of large height gradients, especially where the gradients change sign.

There are no measurements of C_N^2 except at the height of the Lyman α humidiometer (the carriage height), but profiles of the potential refractive index ϕ can be used to estimate C_N^2 from the temperature and wind fields. That is; noting from eq. (11) that $N = (n-1)\times 10^6$,

$$C_n^2 \times 10^{12} = \frac{C_w^2}{\sqrt{\left(\frac{du}{dz}\right)^2 + \left(\frac{dv}{dz}\right)^2}} \left(\frac{d\phi}{dz}\right)^2$$

and

$$C_n^2 \times 10^{12} = \frac{C_T^2}{\left(\frac{d\theta}{dz}\right)^2} \left(\frac{d\phi}{dz}\right)^2 .$$

These calculations are shown in Fig. 16 and should be compared with the carriage-measured values at the carriage height. Clearly, the need for averaging the turbulent quantities between levels to estimate the value at midpoint between levels introduces fairly large errors in the calculated profile of

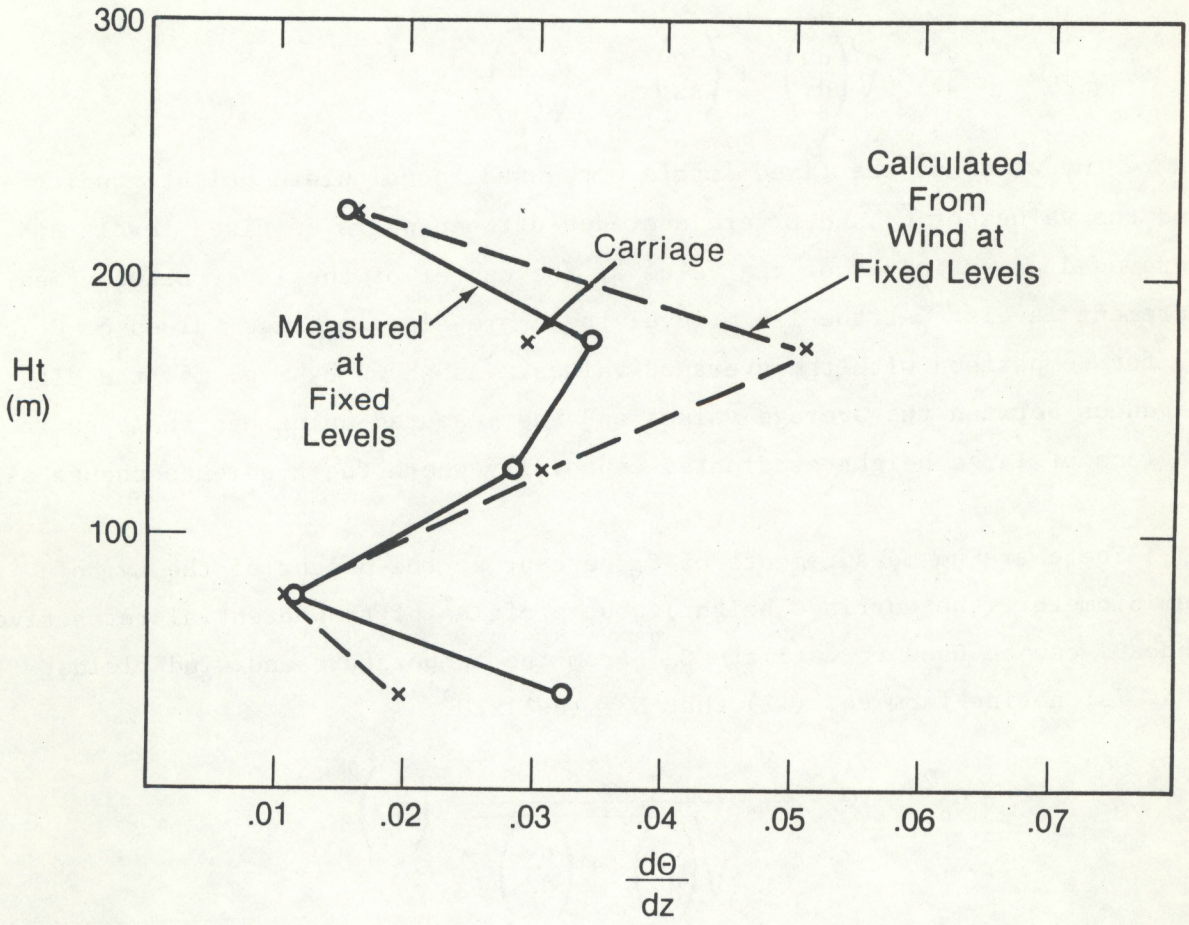

Figure 15.--Measured vs. calculated profiles of potential temperature gradient vs. height at 1812 MST.

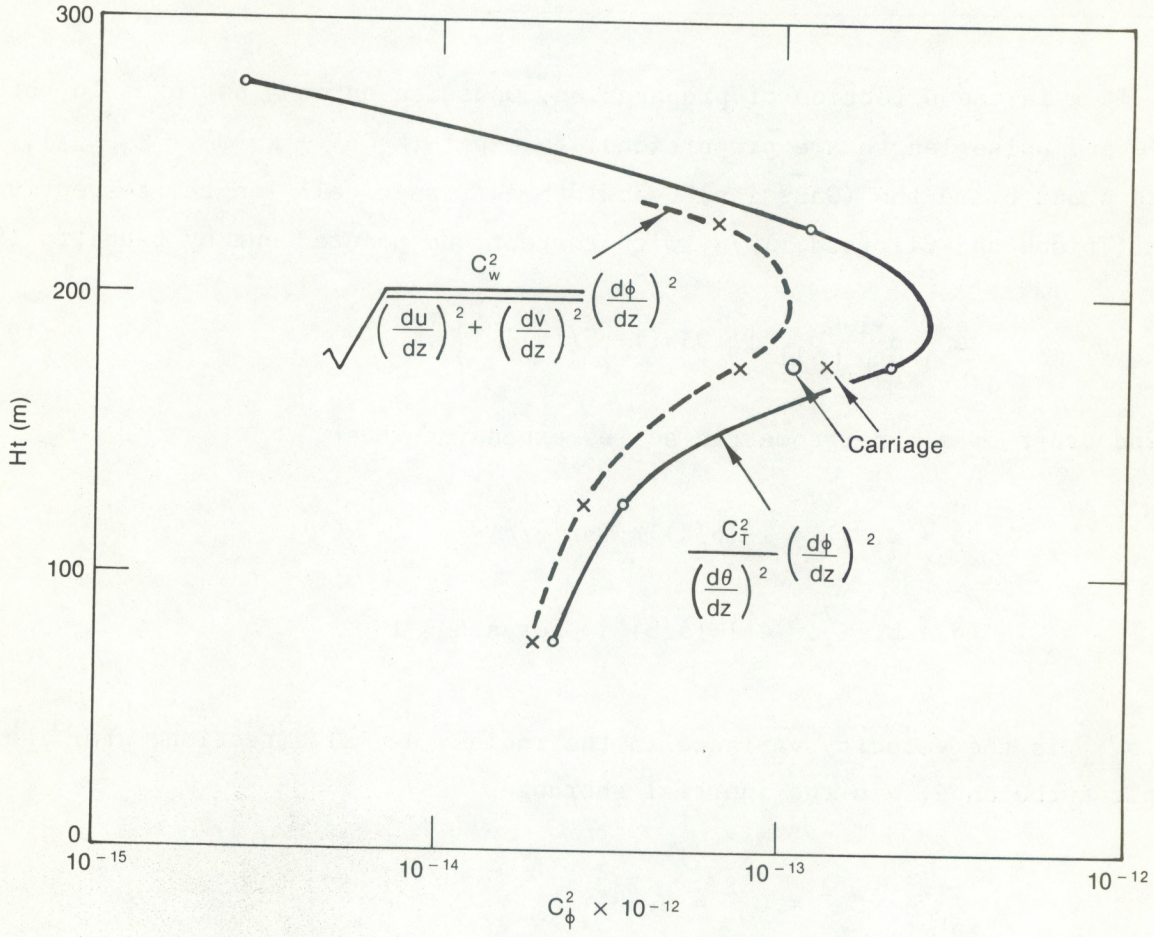

Figure 16.--Measured vs. calculated profiles of potential refractivity gradient vs. height at 1812 MST.

C_n^2, but even so, the layer of high C_n^2 is fairly well represented by measurements of the wind and temperature parameters. In practice the problem would be inverted, and the radar would be used to measure C_w^2 (du/dz) and C_n^2 in order to calculate $d\phi/dz$ or dN/dz.

Calculation of C_w^2 from Doppler Spectral Width

If x is the direction of propagation, Gaussian antenna patterns in both angle and pulse length are proportional to $\exp[-(k_x^2b^2 + k_y^2a^2 + k_z^2a^2)]$, where a and b are the (Gaussian) beamwidth and range cell length, respectively. Then (Frisch and Clifford, 1974, with corrections pointed out by Labbitt, 1979),

$$\varepsilon = \delta^{-1}\left\{\sigma_{11}^2[1.35\alpha(1-\gamma^2/15)]^{-1}\right\}^{3/2} \tag{19}$$

to 2nd order of a hypergeometric series expansion where,

$$\delta = a,\ \gamma^2 = 1-(b/a)^2 \quad \text{for } b/a < 1$$

$$\delta = b,\ \gamma^2 = 4[1-(a/b)^2] \quad \text{for } a/b < 1$$

and σ_{11}^2 is the velocity variance in the radial (say x) direction. For isotropic turbulence, in the inertial subrange,

$$C_u^2 = C_v^2 = C_w^2 = B\varepsilon^{2/3} \tag{20}$$

so

$$C_w^2 = B\delta^{-2/3}\sigma_{11}^2[1.35\alpha(1-\gamma^2/15)]^{-1} \tag{21}$$

where

$$\sigma_{11}^2 = \frac{\int(v_{11}-\bar{v})^2 S(v)dv}{\int S(v)dv}$$

and S(v) is the velocity spectrum observed by the Doppler radar.

Values of ε measured at the 175 m level on the tower are compared with radar-measured values at a height of 200 m (with 100 m resolution) in Fig. 17. These are easily converted to C_w^2 using Eq. (20). Considering the 1500 ft. separation of the radar and the tower these results are considered to be in good agreement. However, there are other cases when the two measurements show very little correlation, and it is too early to say whether the degree of agreement depends on wind direction or some other factor.

Conclusions

The radar measurable quantities, shear, C_w^2 and C_n^2 can be used to deduce height gradients of radio refractive index ($d\phi/dz$) aloft with a considerable degree of accuracy. It remains to be shown that the quantities C_w^2 and C_n^2 measured by the radar are accurate enough for practical application. The accuracy of C_w^2 is especially uncertain because it is obtained from the 2nd moment of the Doppler velocity spectrum and becomes inaccurate for very weak signals. Future plans call for locating the radar closer to the tower, so that temporal changes and spatial inhomogeneity will be less important factors in the comparison of in situ and radar measurements.

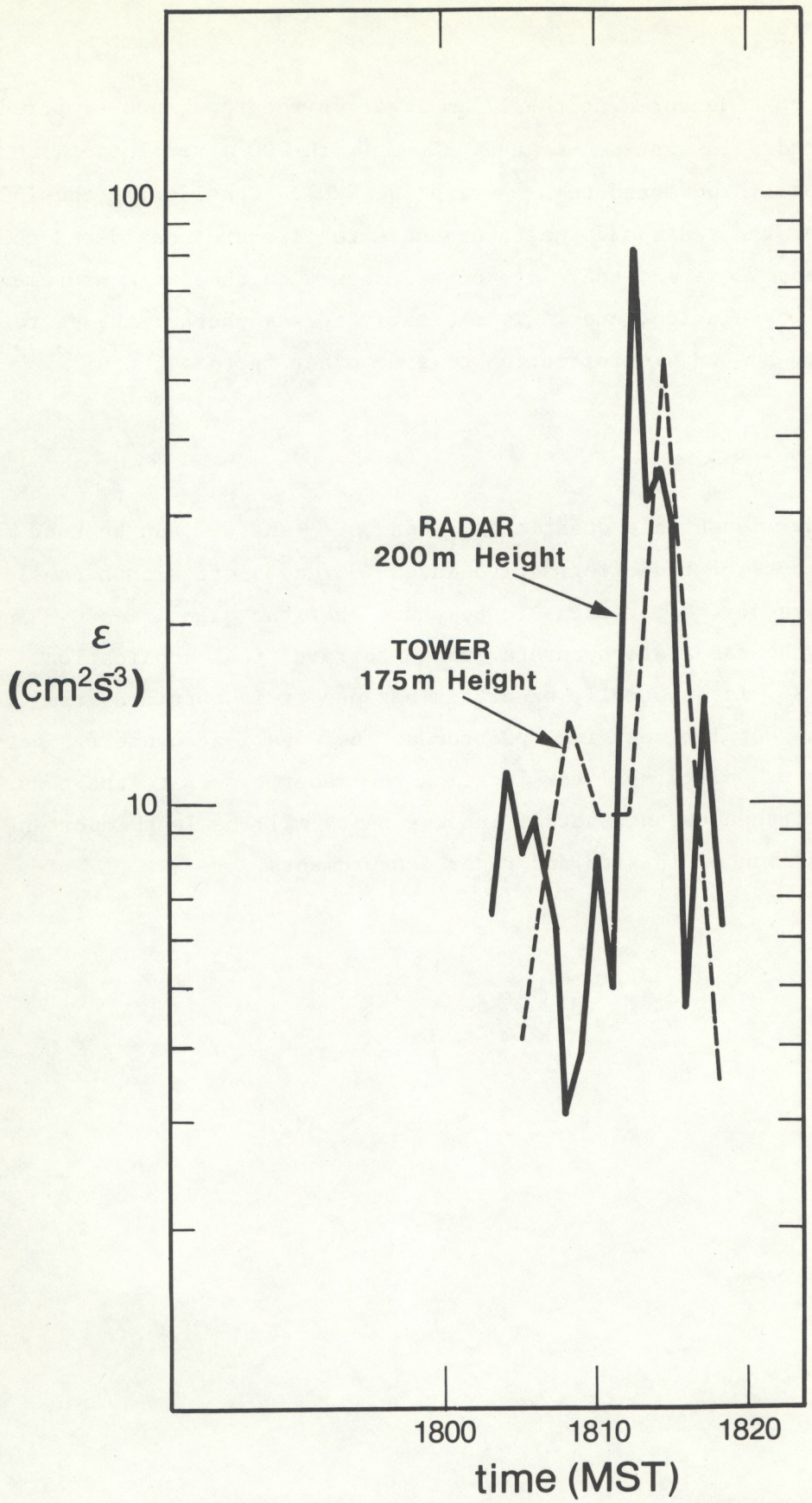

Figure 17.--Tower-measured vs. radar-measured turbulent dissipation rate at the times shown.

REFERENCES

Gossard, E.E., R.B. Chadwick, W.D. Neff, and K.P. Moran (1982): The use of ground-based Doppler radars to measure gradients, fluxes and structure parameters in elevated layers. J. Appl. Meteorol., 21, 211-226.

Labitt, M. (1979): Some basic relations concerning the radar measurement of air turbulence. MIT Lincoln Laboratory, ATC Working Paper No. 46WP-5001, 12 pgs.